Journal of Constructional Steel Research 65 (2009) 542–551

Contents lists available at ScienceDirect

Journal of Constructional Steel Research

journal homepage: www.elsevier.com/locate/jcsr

Natural periods of steel plate shear wall systems

Cem Topkaya *, Can Ozan Kurban

Department of Civil Engineering, Middle East Technical University, 06531 Ankara, Turkey

ARTICLE INFO

Article history:
Received 26 December 2007
Accepted 10 March 2008

Keywords:
Steel plate shear wall
Natural period
Finite element
Period elongation
Simplified formula

ABSTRACT

In most seismic building codes, the design base acceleration is computed using the natural period of vibration of the structure. Design specifications provide empirical formula to estimate the fundamental natural period of a system. In this study a class of steel plate shear walls, that have uniform properties through their height, was considered. The fundamental natural periods of this class of structures were determined using three dimensional geometrically linear finite element analyses and were compared against the estimates provided by seismic design specifications. Comparisons reveal that estimations using approximate formula can lead to unsatisfactory results. Based on this observation a simple hand method has been developed to predict the fundamental period of a steel plate shear wall. In the development of the hand method the steel plate shear wall has been recognized as a vertical cantilever for which simplified analytical solutions exist. Contributions of shear and bending stiffness of the wall have been explicitly taken into account. Furthermore, this simple method has been extended to dual systems having plate walls and special moment frames in the context of theories on wall-frame structures. Natural period estimations using the method that was developed in this study are compared with the finite element solutions and a good agreement is demonstrated. In addition, the effects of geometrical and material nonlinearities on the fundamental period were explored. The fundamental periods of steel plate walls were investigated at various drift levels. Based on the numerical analysis, elongation of the periods due to buckling and yielding of infill plates were quantified and are presented herein.

1. Introduction and background

Steel plate shear walls (SPSW) can be used in buildings to resist forces produced during an earthquake. In a typical SPSW system steel infill plates that are one story high and one bay wide are connected to stiff horizontal and vertical boundary elements (HBE and VBE). The resulting system is a cantilever which resembles a plate girder. Design philosophies for SPSW systems can be divided into two categories. Earlier designs used thick or stiffened plates to prevent buckling due to shear stresses forming at low load levels. Recent designs employ thinner plates and rely on the post buckling capacity. Experimental and numerical studies [1–16] reported to date revealed that SPSW systems have high stiffness, excellent energy absorption capacity and stable hysteresis characteristics.

Most of the seismic building codes [17–19] provide expressions for design base acceleration as a function of the natural period of the structure. Therefore, accurate computation of the fundamental natural period has paramount importance in determining the magnitude of lateral forces in design.

For determination of the fundamental period of vibration of the structure, expressions based on methods of structural dynamics (for example Rayleigh's method or computer based eigenvalue analysis) are permitted by design specifications such as ASCE 7 [17], Eurocode 8 [18], and National Building Code of Canada (NBCC) [19]. In addition, design specifications provide empirical formulas to estimate the fundamental period of the structure. Usually, these formulas depend on the type of the structural system, materials used, and the gross dimensions. Traditionally, code period expressions have been derived or validated using measured building periods during earthquakes [20,21]. These expressions are generally adjusted to give lower-bound estimates so that design seismic forces are not underestimated. There are two main uses for these empirical formulas. First, these period formulas are useful in design as the actual structure period is not known before a first trial design is performed. Second, in design codes such as ASCE 7 [17] and NBCC [19], these approximate formulas together with a coefficient are used to provide an upper limit on the fundamental period calculated based on the methods of structural dynamics. In NBCC [19] it is specified that for shear walls the value obtained by such methods not exceed 2.0 times the value determined by empirical expressions. Similarly, in ASCE 7 [17] the basic period can be increased up to 1.4 times for high seismic zones and to 1.7 times for low seismic zones. These restrictions are imposed to safeguard against unreasonable assumptions in the methods of structural dynamics, which may lead to unreasonably long periods and hence unconservative values of base shear.

* Corresponding author. Tel.: +90 312 210 5462; fax: +90 312 210 7991.
E-mail address: ctopkaya@metu.edu.tr (C. Topkaya).

0143-974X/$ – see front matter © 2008 Elsevier Ltd. All rights reserved.
doi:10.1016/j.jcsr.2008.03.006

According to design specifications ASCE 7 [17] as developed in AISC Seismic Provisions for Structural Steel Buildings [22], EC 8 [18], and NBCC [19], the fundamental period of vibration (T) of an SPSW system can be found by:

$$T = 0.05H^{3/4} \tag{1}$$

where; H: height of the building in meters.

In this paper, the accuracy of the empirical equations given by the design specifications is assessed. For assessment a class of structures with steel plate shear walls possessing different geometrical and mass properties was selected. The fundamental natural periods of these structures were determined using three dimensional geometrically linear finite element analyses. The values obtained from numerical analysis were compared against the approximations provided by design specifications. Next, a practical hand method is developed to estimate the natural period of SPSW systems. This method is based on the premise that the SPSW is a shear weak vertical cantilever, for which approximate analytical solutions exist. The formulation of this practical method is presented and its accuracy is assessed by making comparisons with finite element results. Finally, the period elongation due to buckling and yielding of infill plates is explored. Structures were subjected to various drift levels and elongation in fundamental period due to buckling and yielding was computed by making use of numerical analysis. The details of the finite element procedure are explained and the results from these analyses are presented.

2. Assessment of the empirical equation presented in design specifications

In order to make an assessment of code recommendations, a class of structures was considered. Two typical floor plans shown in Fig. 1 were used for this assessment. Perimeter frames and walls in the N-S direction were designed according to the recommendations given in AISC Provisions for Structural Steel Buildings [23] and AISC Seismic Provisions [22]. Two different lateral load resisting systems were considered. In the first one, it was assumed that the perimeter framing has pinned beam to column connections and the steel plate wall is used as the sole lateral load resisting system. In the second one, it was assumed that the perimeter framing has rigid beam to column connections and the dual system (wall-frame) is used as a lateral load resisting system. In both lateral load resisting systems HBE to VBE connections were assumed rigid.

In order to cover a wide range of slenderness and aspect ratios, infill plate thickness values of 3.0 mm and 6.0 mm and plate aspect ratios of 1 and 2 were considered. These values are within the bounds recommended by AISC Seismic Provisions [22]. For all structures, the clear height between HBE was taken as 3 m. A dead load of 4.4 kN/m^2 and a live load of 2 kN/m^2 were considered during the design. Mass per story including the reduced live load was 0.5 tons/m^2. According to these assumptions, mass per story for each perimeter frame was taken as 150 tons for 3 bay structures (Floor Plan 1) and 250 tons for 5 bay structures (Floor Plan 2). For plate walls 2,4,6,8,10 story structures were considered. For dual systems 2,4,6,8,10,15,20,25,30,35,40 story structures were considered. For plate wall only systems, no more than 10 stories was considered because the height of these structures designed per seismic category F of AISC Seismic Provisions [22] is limited to 30 m. A total of 40 steel plate walls and 88 dual systems were designed according to capacity design principles and the details of the sections are given in Tables 1 and 2.

Fundamental natural periods of this class of structures were determined using three dimensional finite element analyses. Infill plates, VBE, HBE, beams and columns were modeled using 8-node shell elements. Lumped masses were placed at story levels.

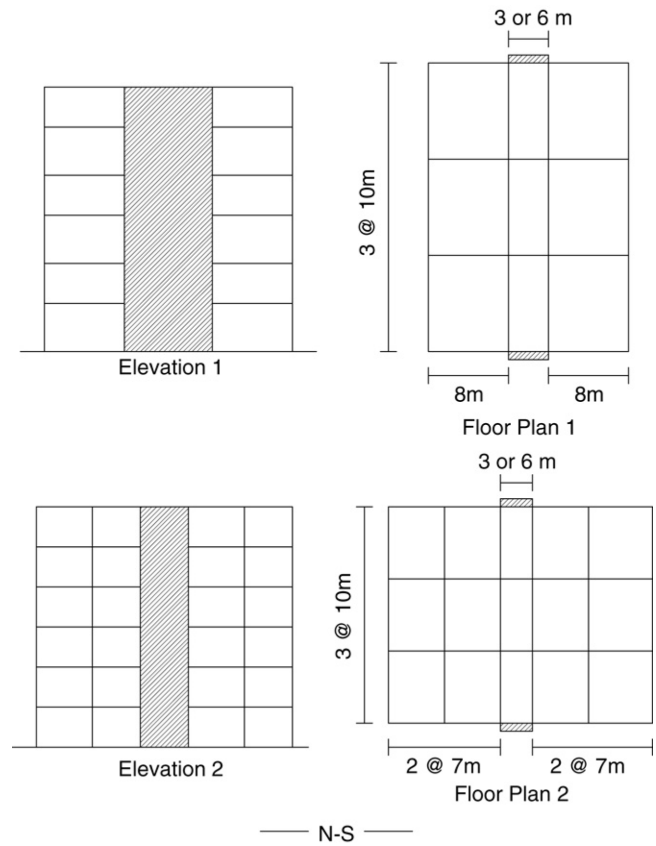

Fig. 1. Floor plans.

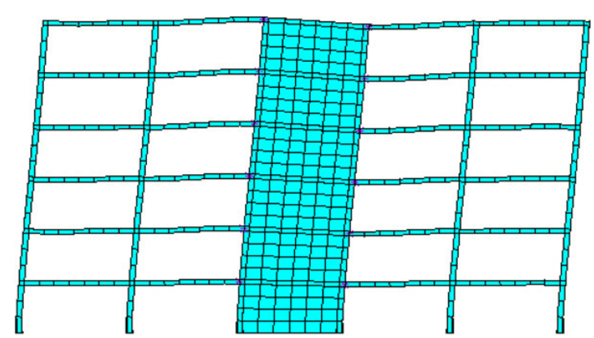

Fig. 2. A typical finite element mesh and fundamental mode of vibration.

A commercially available finite element program ANSYS [24] was used to conduct the analysis. An eigenvalue analysis was performed for each case to determine the fundamental natural period of vibration. A typical finite element mesh displaying the fundamental mode of vibration is given in Fig. 2.

Natural period values determined using finite element analysis are given in Tables 1 and 2. The periods found using the empirical Eq. (1) were normalized with the results from the finite element analysis and are presented in Figs. 3a and c. In these figures, analysis cases are sorted so that the estimates are plotted in descending order. According to Fig. 3a period estimations using Eq. (1) produce overestimations (unconservative results) for 6 cases out of 40 plate walls, and for 5 cases out of 88 dual systems. The statistical measures related with the period estimates are given in Table 3. According to the statistical measures and Fig. 3c there are large discrepancies between the estimates and the numerical solution for dual systems. The upper limit provided by the design specifications were evaluated by comparing the lengthened periods and the periods from numerical analysis. For

Table 1
Properties of wall systems

Case	# of story	Plate thickness (mm)	Plate width (m)	Floor plan	VBE section HD	Period (s)	Case	# of story	Plate thickness (mm)	Plate width (m)	Floor plan	VBE section HD	Period (s)
1	2	3	3	1	320 × 158	0.289	21	6	6	3	1	400 × 744	0.645
2	2	3	3	2	320 × 158	0.373	22	6	6	3	2	400 × 744	0.832
3	2	3	6	1	320 × 158	0.203	23	6	6	6	1	400 × 744	0.412
4	2	3	6	2	320 × 158	0.262	24	6	6	6	2	400 × 744	0.532
5	2	6	3	1	400 × 287	0.208	25	8	3	3	1	400 × 509	1.285
6	2	6	3	2	400 × 287	0.268	26	8	3	3	2	400 × 509	1.660
7	2	6	6	1	400 × 287	0.148	27	8	3	6	1	400 × 509	0.796
8	2	6	6	2	400 × 287	0.191	28	8	3	6	2	400 × 509	1.028
9	4	3	3	1	400 × 287	0.563	29	8	6	3	1	400 × 990	0.901
10	4	3	3	2	400 × 287	0.727	30	8	6	3	2	400 × 990	1.163
11	4	3	6	1	400 × 287	0.373	31	8	6	6	1	400 × 990	0.564
12	4	3	6	2	400 × 287	0.481	32	8	6	6	2	400 × 990	0.728
13	4	6	3	1	400 × 551	0.402	33	10	3	3	1	400 × 634	1.692
14	4	6	3	2	400 × 551	0.518	34	10	3	3	2	400 × 634	2.185
15	4	6	6	1	400 × 551	0.267	35	10	3	6	1	400 × 634	1.032
16	4	6	6	2	400 × 551	0.345	36	10	3	6	2	400 × 634	1.332
17	6	3	3	1	400 × 421	0.885	37	10	6	3	1	BUILT UP	1.196
18	6	3	3	2	400 × 421	1.143	38	10	6	3	2	BUILT UP	1.544
19	6	3	6	1	400 × 421	0.567	39	10	6	6	1	BUILT UP	0.735
20	6	3	6	2	400 × 421	0.731	40	10	6	6	2	BUILT UP	0.949

All HBE are HEA 300. (BUILT UP section depth = 580 mm, flange width = 475 mm, flange thickness = 130 mm, web thickness = 90 mm).

Table 2
Properties of dual systems

Case	# of story	Plate T. (mm)	Plate W. (m)	Floor plan	VBE and column section HD	Period (s)	Case	# of story	Plate T. (mm)	Plate W. (m)	Floor plan	VBE and column section HD	Period (s)
1	2	3	3	1	320 × 198	0.242	45	2	3	3	2	320 × 198	0.297
2	2	3	6	1	320 × 198	0.179	46	2	3	6	2	320 × 198	0.225
3	2	6	3	1	320 × 198	0.203	47	2	6	3	2	320 × 198	0.253
4	2	6	6	1	320 × 198	0.142	48	2	6	6	2	320 × 198	0.180
5	4	3	3	1	320 × 198	0.529	49	4	3	3	2	320 × 198	0.647
6	4	3	6	1	320 × 198	0.368	50	4	3	6	2	320 × 198	0.463
7	4	6	3	1	320 × 198	0.472	51	4	6	3	2	320 × 198	0.584
8	4	6	6	1	320 × 198	0.309	52	4	6	6	2	320 × 198	0.392
9	6	3	3	1	320 × 198	0.880	53	6	3	3	2	320 × 198	1.064
10	6	3	6	1	320 × 198	0.606	54	6	3	6	2	320 × 198	0.758
11	6	6	3	1	320 × 198	0.813	55	6	6	3	2	320 × 198	0.990
12	6	6	6	1	320 × 198	0.530	56	6	6	6	2	320 × 198	0.668
13	8	3	3	1	320 × 198	1.272	57	8	3	3	2	320 × 198	1.518
14	8	3	6	1	320 × 198	0.885	58	8	3	6	2	320 × 198	1.098
15	8	6	3	1	320 × 198	1.196	59	8	6	3	2	320 × 198	1.437
16	8	6	6	1	320 × 198	0.796	60	8	6	6	2	320 × 198	0.994
17	10	3	3	1	320 × 198	1.692	61	10	3	3	2	320 × 198	1.996
18	10	3	6	1	320 × 198	1.196	62	10	3	6	2	320 × 198	1.470
19	10	6	3	1	320 × 198	1.608	63	10	6	3	2	320 × 198	1.907
20	10	6	6	1	320 × 198	1.095	64	10	6	6	2	320 × 198	1.354
21	15	3	3	1	320 × 198	2.833	65	15	3	3	2	320 × 198	3.264
22	15	3	6	1	320 × 198	2.075	66	15	3	6	2	320 × 198	2.493
23	15	6	3	1	320 × 198	2.740	67	15	6	3	2	320 × 198	3.163
24	15	6	6	1	320 × 198	1.953	68	15	6	6	2	320 × 198	2.355
25	20	3	3	1	400 × 216	4.000	69	20	3	3	2	400 × 216	4.496
26	20	3	6	1	400 × 216	3.003	70	20	3	6	2	400 × 216	3.519
27	20	6	3	1	400 × 216	3.891	71	20	6	3	2	400 × 216	4.388
28	20	6	6	1	400 × 216	2.865	72	20	6	6	2	400 × 216	3.365
29	25	3	3	1	400 × 237	5.208	73	25	3	3	2	400 × 237	5.725
30	25	3	6	1	400 × 237	3.984	74	25	3	6	2	400 × 237	4.564
31	25	6	3	1	400 × 237	5.102	75	25	6	3	2	400 × 237	5.612
32	25	6	6	1	400 × 237	3.831	76	25	6	6	2	400 × 237	4.400
33	30	3	3	1	400 × 262	6.410	77	30	3	3	2	400 × 262	6.900
34	30	3	6	1	400 × 262	4.975	78	30	3	6	2	400 × 262	5.584
35	30	6	3	1	400 × 262	6.289	79	30	6	3	2	400 × 262	6.785
36	30	6	6	1	400 × 262	4.808	80	30	6	6	2	400 × 262	5.412
37	35	3	3	1	400 × 287	7.692	81	35	3	3	2	400 × 287	8.105
38	35	3	6	1	400 × 287	6.024	82	35	3	6	2	400 × 287	6.637
39	35	6	3	1	400 × 287	7.576	83	35	6	3	2	400 × 287	7.987
40	35	6	6	1	400 × 287	5.882	84	35	6	6	2	400 × 287	6.460
41	40	3	3	1	400 × 347	8.696	85	40	3	3	2	400 × 347	8.995
42	40	3	6	1	400 × 347	6.897	86	40	3	6	2	400 × 347	7.441
43	40	6	3	1	400 × 347	8.621	87	40	6	3	2	400 × 347	8.879
44	40	6	6	1	400 × 347	6.711	88	40	6	6	2	400 × 347	7.263

All HBE are HEA300, Beams HEA450 for Floor plan 1, and HEA400 for Floor plan 2.

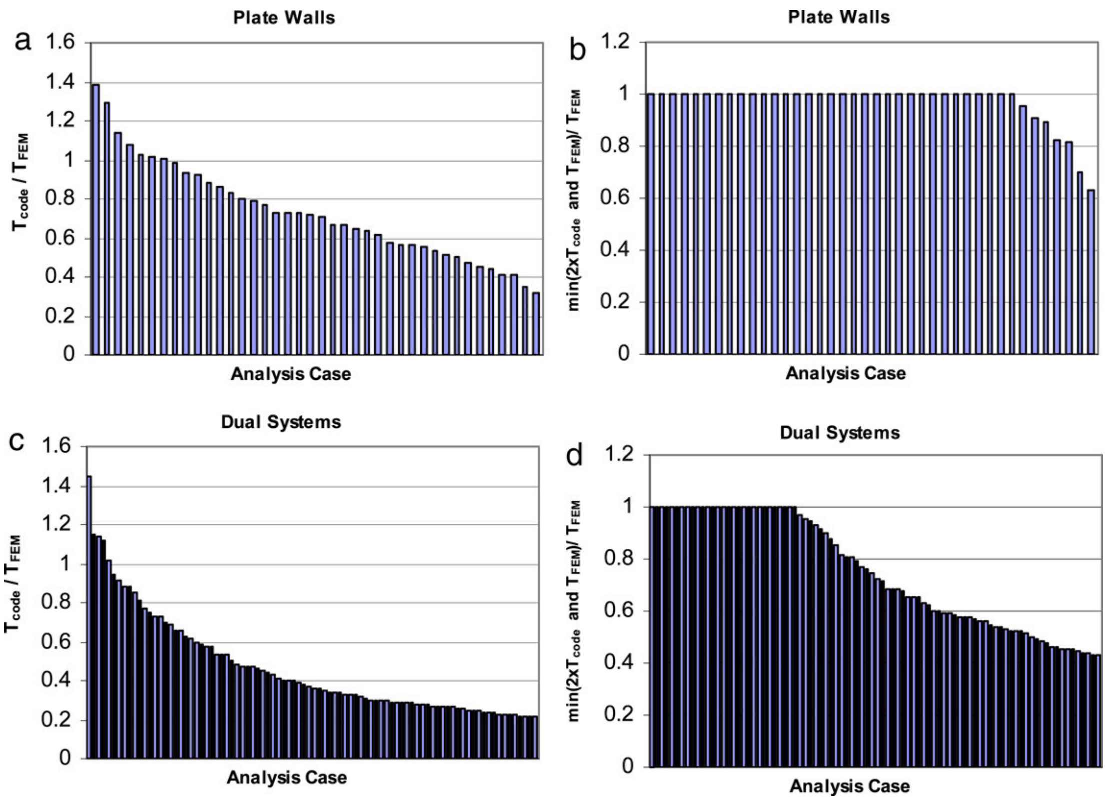

Fig. 3. Comparison of specification equation estimates with finite element results.

Table 3
Statistical measures of estimates

	Period normalized by period from finite element analysis			
	Plate walls		Dual systems	
	Eq. (1)	Hand method	Eq. (1)	Hand method
Average	0.73	1.06	0.47	1.00
Standard deviation	0.25	0.04	0.26	0.05
Maximum	1.39	1.16	1.45	1.15
Minimum	0.31	1.02	0.22	0.92

cases where the estimations from the empirical equation produce unconservative results, period values from numerical solution can be used in design. For others, the estimates were multiplied by 2.0 as recommended by NBCC [19] and smaller of the lengthened period and the period from numerical solution was used to determine the governing one. Fig. 3b and d show the governing cases when the upper limit is applied to the period estimation equation. According to these figures for 33 cases out of 40 plate walls period values from numerical solution can be used in design and for 7 cases the upper limit on the period governs the design. Similarly, for 29 cases out of 88 dual systems period values from numerical solution can be used in design while 59 cases are governed by the upper limit.

3. Development of a simple hand method for fundamental period estimation of steel plate walls

A simple hand method is formulated herein to be used for estimation of fundamental natural periods of steel plate shear walls. This formulation is based on the observation that the SPSW acts as a vertical cantilever. Both bending and shear deformations have to be taken into account to accurately model the physical system. Equation of motion for a cantilever with shear deformation and rotational inertia effects is expressed with the following equation [25,26]:

$$m\frac{\partial^2 u}{\partial t^2} + EI_w\frac{\partial^4 u}{\partial x^4} - mr^2\left(1+\frac{E}{KG}\right)\frac{\partial^4 u}{\partial x^2\partial t^2} + \frac{m^2r^2}{KGA_w}\frac{\partial^4 u}{\partial t^4} = 0 \qquad (2)$$

where; m: mass per unit height of the wall (constant), E: modulus of elasticity, G: shear modulus, I_w: second moment of area of the wall with respect to the neutral axis, K: shear constant, A_w: area of the wall, r: radius of gyration of SPSW cross section, x: distance along height of the wall, u: lateral displacement of the wall.

Usually numerical techniques are used for the solution of Eq. (2) to obtain natural periods. There are approximate solutions [27] for some special cases that neglect rotational inertia effects. However, these solutions are lengthy and are not practical for design purposes.

On the other hand, Souhwell-Dunkerley [28] approximation (Eq. (3)) can be used to estimate the fundamental natural period of the wall. In this approximation, the fundamental natural period (T_w) of the wall is expressed in terms of the cyclic natural frequencies, f_b and f_s, of two cantilevers, one deforming in bending and the other one in shear, respectively.

$$T_w \approx \sqrt{\frac{1}{f_b^2}+\frac{1}{f_s^2}}. \qquad (3)$$

Cyclic natural frequency of a cantilever deforming in bending can be found by:

Table 4
r_f factors proposed by Zalka [29] as a function of number of stories

# of story n	1	2	3	4	5	6	7	8	9	10	11
r_f	0.493	0.653	0.770	0.812	0.842	0.863	0.879	0.892	0.902	0.911	0.918
# of story n	12	13	14	15	16	18	20	25	30	50	
r_f	0.924	0.929	0.934	0.938	0.941	0.947	0.952	0.961	0.967	0.980	

$$f_b = r_f \frac{0.5595}{H^2}\sqrt{\frac{EI_w}{m}}. \tag{4}$$

In Eq. (4) r_f is a factor proposed by Zalka [29] that takes the contribution of lumped masses at story levels into account. Actually, the frequency expression is derived for a beam with uniform mass and the solution is further modified using the r_f factor to include the effects of lumped masses. The r_f factors proposed by Zalka [29] are given in Table 4.

Similarly, cyclic natural frequency of a cantilever deforming in shear can be found by:

$$f_s = r_f \frac{1}{4H}\sqrt{\frac{KGA_w}{m}}. \tag{5}$$

Same set of r_f factors given in Table 4 is used for the cantilever deforming in shear.

At this point, in order to compute the natural frequency of a cantilever deforming in shear, one has to know the shear factor (K) for the SPSW cross section. Shear factors (K) for such cross sections are not readily available. By definition the effective shear area (KA_w) is computed as follows [30]:

$$KA_w = \frac{I_w^2}{\beta} \qquad \beta = \int_{A_w} \frac{Q^2}{b^2}\mathrm{d}A \tag{6}$$

where, Q: statical moment of the area with respect to the neutral axis, b: width of the section.

The exact calculation of β requires the integration of fourth order polynomials that might be cumbersome during routine design practice. However, Atasoy [31] developed a simpler approximation for computation of β by assuming linear variation of Q/b along continuity regions. In this approximation, the contribution from vertical boundary elements (β_1) and the one from the infill plate (β_2) are added together as follows:

$$\begin{aligned} &\beta = \beta_1 + \beta_2 \\ &\beta_1 = \frac{Q_1^2 + Q_2^2}{t_w} d_{\mathrm{VBE}} \qquad \beta_2 = \frac{Q_3^2 + Q_4^2}{2ptk} plw \\ &Q_1 = A_{fl}(0.5plw + d_{\mathrm{VBE}}) \\ &Q_2 = Q_1 + A_{\mathrm{web}} 0.5(plw + d_{\mathrm{VBE}}) \\ &Q_3 = A_{\mathrm{VBE}} 0.5(plw + d_{\mathrm{VBE}}) \\ &Q_4 = Q_3 + \frac{(plw)^2}{8} ptk \end{aligned} \tag{7}$$

where, plw: width of the infill plate, ptk: thickness of the infill plate, d_{VBE}: depth of VBE section, t_w: thickness of VBE web, A_{fl}: area of VBE flange, A_{web}: area of VBE web, A_{VBE}: area of VBE.

It should be emphasized that β_2 is much larger compared to β_1 for typical steel plate shear wall geometries.

The accuracy of the developed hand method is checked by making use of the 40 walls details of which are given earlier. The natural periods obtained using this hand method are compared against the finite element solutions in Fig. 4. It is evident from this figure that the hand method provides excellent estimations when compared with the numerical solution. Statistical measures for the estimates are given in Table 3. An example problem is presented in the Appendix.

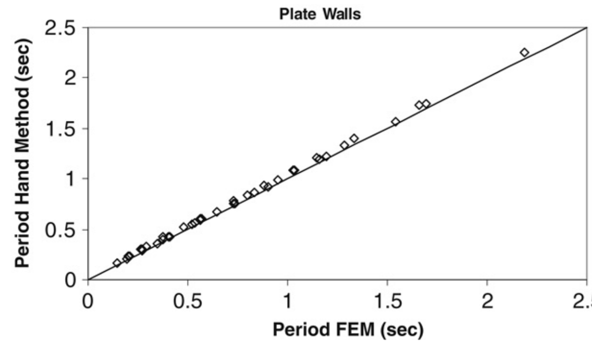

Fig. 4. Comparison of the hand method estimates with finite element results (Plate walls).

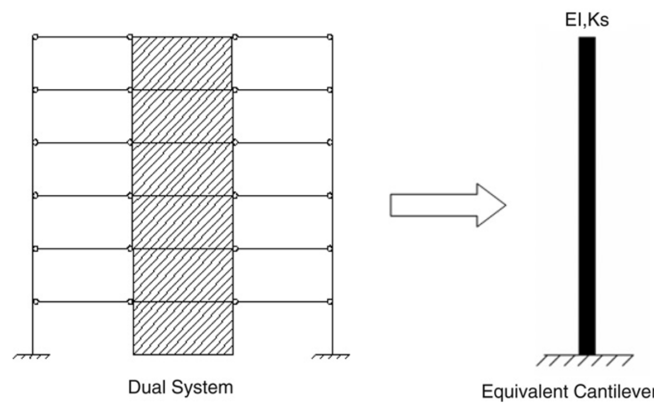

Fig. 5. Wall-frame structure idealized as a shear-flexure cantilever.

4. Natural period estimation of dual systems

Natural period estimation of wall-frame structures has been studied in the past [29,32–35]. Theorems developed for wall frame structures can be coupled with the hand method developed in the previous section to calculate the natural period of steel plate shear wall systems with moment resisting frames. As shown in Fig. 5, the idea is to idealize the wall frame structure as an equivalent shear-flexure cantilever. Bending and shear rigidity of the equivalent shear-flexure cantilever need to be determined from the properties of the wall frame system. The bending rigidity (EI) of the coupled system is influenced by the bending rigidity of the walls and that of the columns. One also has to account for the reduction in bending rigidity of the wall due to shear deformations. This can be included into the analysis by considering the method developed in the previous section. For each wall that is a part of the lateral load resisting system a modified second moment of area, I_{mw}, is defined as follows:

$$I_{mw} = \frac{mH^4}{0.313 r_f^2 T_w^2 E} \tag{8}$$

where, T_w: fundamental natural period of the wall itself calculated using the principles outlined earlier.

The bending rigidity of the equivalent shear-flexure cantilever is then calculated as:

$$EI = \sum EI_{mw} + \sum EI_c \tag{9}$$

where, I_c: second moment of area of column.

It should be noted that the term due to second moment of area of columns is much smaller compared to the counterpart due to second moment of area of the walls and can therefore be neglected for practical cases.

The shear rigidity per story (K_s) of the framing can be calculated by considering the contributions of the columns and beams [33]. At this point, it should be recognized that beams that belong to the bays adjacent to the wall require a special treatment. Due to the stiff end sections, rigidity of these beams is treated separately from the rest of the framing system. According to this observation, shear rigidity per story (K_s) can be calculated as follows:

$$K_s = \xi(K_{s1} + K_{s2}) \tag{10}$$

where,

$$K_{s1} = \frac{12E}{h\left[\frac{1}{\Sigma\left(\frac{I_c}{h}\right)_i} + \frac{1}{\Sigma\left(\frac{I_b}{L}\right)_j}\right]} \tag{11}$$

$$K_{s2} = \sum\left(\frac{6EI_b}{Lh}\left[(1+r)(1+2r+s)\right]\right)_i \tag{12}$$

in which $r = \dfrac{plw}{2L_b}$ $\quad s = \dfrac{\eta - 3r - 1}{\eta + 2}$ $\quad \eta = \dfrac{6I_cL}{I_bh}$

where, h: story height, I_b: second moment of area of beam, L: length of beam.

In Eq. (10), K_{s1} represents the rigidity of the framing excluding the beams adjacent to the wall and K_{s2} represents the rigidity of beams that are adjacent to the wall. The summation of these rigidities is modified by an efficiency factor [29] ξ to account for the reduction in stiffness due to full height bending of the frame as follows:

$$\xi = \frac{f_{fb}^2}{f_{fb}^2 + f_{fs}^2} \quad \text{where } f_{fs}^2 = \frac{r_f^2\,(K_{s1} + K_{s2})}{(4H)^2\, m} \qquad f_{fb}^2 = \frac{0.313 r_f^2 EI_g}{H^4 m} \tag{13}$$

in which $I_g = \sum A_c d^2$

where, I_g: global second moment of the column and wall sectional areas acting about a common centroid, A_c: cross sectional area of column, d: distance of column to the centroid.

The efficiency factor, ξ, is used to take the axial deformations of columns of the framing into account. Reduction due to axial deformations is significant for narrow and tall structures. For short frames, this factor can be safely neglected and using $\xi = 1$ for all cases result in an underestimation of the fundamental period.

The governing differential equation of the equivalent cantilever can be written as follows [29]:

$$r_f EI\frac{\partial^4 u}{\partial x^4} - r_f K_s \frac{\partial^2 u}{\partial x^2} + m\frac{\partial^2 u}{\partial t^2} = 0. \tag{14}$$

The solution of the differential equation yields the following expression for the fundamental natural period of the system (T_{sys}):

$$T_{\mathrm{sys}} = \frac{2\pi}{\lambda_{sf}^2 r_f}\sqrt{\frac{m}{EI}} \tag{15}$$

where, λ_{sf}: eigenvalue of the problem.

The eigenvalue of this problem is dependent on the relative values of the shear and bending rigidities. The ratio of shear and bending rigidities can be expressed by a factor α where:

$$\alpha = \sqrt{\frac{K_s}{EI}}. \tag{16}$$

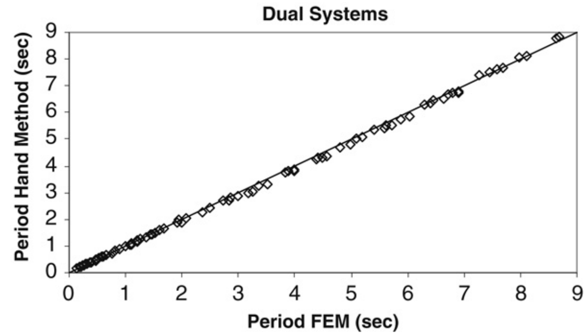

Fig. 6. Comparison of the hand method estimates with finite element results (Dual systems).

The eigenvalue (λ_{sf}) can be found by solving the following expression [33]:

$$2 + \left[\left(\frac{\lambda_1}{\lambda_2}\right)^2 + \left(\frac{\lambda_2}{\lambda_1}\right)^2\right]\cos\lambda_1 H\cosh\lambda_2 H + \left[\frac{\lambda_2}{\lambda_1} - \frac{\lambda_1}{\lambda_2}\right]\sin\lambda_1 H\sinh\lambda_2 H = 0 \tag{17}$$

for which

$$\lambda_2^2 = \lambda_1^2 + \alpha^2$$
$$\lambda_{sf}^4 = \lambda_1^2\lambda_2^2.$$

Approximate solutions of Eq. (17) can be found by [33]:

$$\begin{aligned}(\lambda_{sf}H)^2 &\approx (1.875)^2\left[1 + \frac{\alpha H}{1.875}\right]^{1/2} \quad \alpha H < 6\\ (\lambda_{sf}H)^2 &\approx \frac{\pi}{2}\left[1 + \alpha H\right] \quad \alpha H \geqslant 6.\end{aligned} \tag{18}$$

This method for wall-frame structures was applied to 88 dual systems investigated in this paper. The eigenvalue (λ_{sf}) was found by solving Eq. (17). Fig. 6 presents the comparisons of finite element solution with the hand method proposed herein. Comparisons reveal that combining the findings of the previous section with the theories on wall-frame structures yield in a simple method to accurately calculate the fundamental natural period of dual systems. The statistical measures of the estimates are given in Table 3. An example problem is presented in the Appendix.

5. Effect of geometrical nonlinearities

All of the analysis presented so far was conducted under the premise that infill plates do not buckle under lateral loads. In other words, undeformed geometry was used in the analysis to calculate the natural period of steel plate walls. Geometrically linear analysis can be acceptable for walls with thick plates or stiffened walls. On the other hand, for walls with thin infill plates that encompass a wide range of structures built nowadays this assumption is not realistic. In walls with thin infill plates the slenderness of the plate (short dimension/thickness) can be in the range of 500 to 2000. For such slenderness values the infill plates buckle at very low stresses. Buckling of infill plates occurs at very low lateral loads or due to gravity even before the application of lateral loads. Therefore, in practice a perfectly flat plate is not encountered. Design engineers have to be aware of the implications of having a buckled infill plate as a part of the lateral load resisting system. It was shown by Wagner [36] that buckling of infill plates does not necessarily limit the structural usefulness. The infill plate has significant post buckling strength and stiffness due to formation of tension field action. The post buckled stiffness of the infill plate contributes to the lateral load resistance.

Based on this discussion, it is apparent that a more realistic estimate of the fundamental natural period of a steel plate wall is found by considering the post buckled stiffness of the infill plate rather than the original pre-buckled one. In order to investigate the effects of buckled infill plates on the fundamental natural period, the aforementioned 20 steel plate shear walls which were a part of Floor Plan 1 in Fig. 1 were considered. These systems were analyzed using the finite element method with a special procedure to include buckling of infill plates. This special procedure is essentially an eigenvalue analysis that takes into account the prestressing effects. In this kind of an analysis, first quasi-static loads are applied to the structure and the structure is analyzed by considering geometrical nonlinearities. Second, by making use of the instantaneous stiffness under the set of stresses forming due to quasi-static loads, an eigenvalue buckling analysis is performed. The procedure adopted in this paper to find an eigen solution at a reduced stiffness is not rigorous. Several assumptions related with the geometrical imperfections, type and magnitude of lateral loading are needed. The results are influenced by these analysis assumptions.

Initial imperfections need to be introduced into finite element analysis for modeling buckled infill plates. For this reason a plate center imperfection of 3 mm was considered in all analysis for all stories. It was found by Behbahanifard et al. [37] that the amount of initial imperfection has effects on the lateral stiffness, but this effect is much more pronounced for larger imperfection values that are out of the bounds dictated by construction tolerances. Therefore, considering an imperfection value of 3 mm is within the limit developed by Behbahanifard et al. [37]. In addition, preliminary analysis revealed that considering other imperfection values in the vicinity of 3 mm does not significantly alter the results on the fundamental natural period of the system.

For a particular wall geometry of interest, the first mode of vibration was determined using finite element analysis. Then the wall was loaded laterally with concentrated loads at the story levels with a distribution along the height determined according to the first mode of the structure. A geometrically nonlinear analysis was conducted under these lateral loads. Newton–Raphson method was used to trace the displacement history. The value of the natural period is dependent on the magnitude of lateral forces because the structural behavior deviates from a linear behavior and the tangent stiffness is a function of the amount lateral drift. For all wall systems, lateral loads were applied until the top story drift reaches 0.3%. This drift threshold was determined by observing drift levels at first yield in experiments [15] conducted. In addition, for a maximum drift of 2% including inelastic action, the maximum allowed elastic drift is calculated as 0.3% if a displacement amplification (C_d) value of 6 is used as recommended by AISC Seismic Provisions [22]. After the wall system has been subjected to a top drift of 0.3%, an eigenvalue analysis that takes the pre-stressing effects into account was conducted to determine the natural period.

Natural period of twenty structures were computed using the outlined method. Typical first mode of vibration of an SPSW system is presented in Fig. 7 and the buckling of infill plates is displayed in this figure. Obviously, as a result of the reduction in lateral stiffness, an elongation in period was observed. Results of these analyses are presented in Fig. 8. In this figure, the period of the system considering post buckled plates is normalized by the period of the wall without considering buckling. It is evident from this figure that the period elongation due to early buckling of infill plates is not pronounced. The maximum amount of period elongation stayed under 30% and was observed for 2 story structures. As the height of the structure increases, bending deformations dominate over the shear deformations; with this effect the amount of period elongation decreases with the height of the system. Lower values of period elongation are due to the presence of stiff vertical boundary members that contribute significantly to the bending and shear stiffness. Although infill plates buckle and exhibit a more flexible response, their contribution to the overall stiffness is lower when compared with the stiffness provided by the boundary members that remain intact. Furthermore, the general use of the square root of the stiffness during the calculation of natural period further reduces the importance of reduction in stiffness. The average elongation in period for the systems investigated is 17%. Based on these observations, it is recommended that the effect of buckled infill plates be neglected in determining the natural period of the wall. Hence, the hand method proposed in this paper is sufficient for design purposes. If a more precise value for the period is required, then an eigenvalue analysis including geometrical nonlinearities can be conducted or the period value obtained from linear analysis can be increased by 15% to accommodate for the period elongation. It should also be noted that neglecting geometrical nonlinearities in determining natural period results in conservative designs.

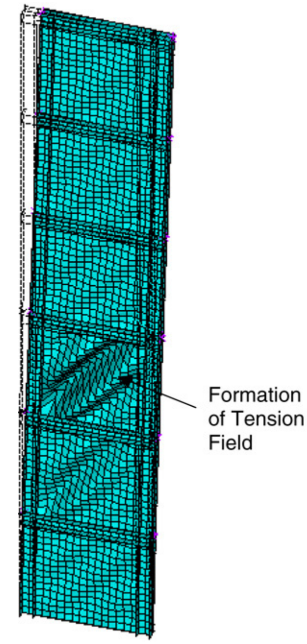

Fig. 7. Fundamental vibration mode of a steel plate wall with buckled infill plates.

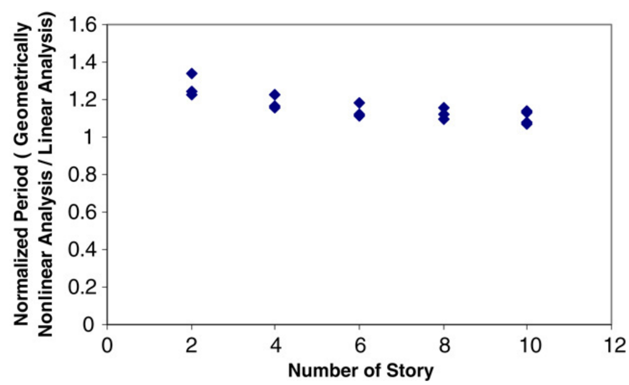

Fig. 8. Effects of geometrical nonlinearities on fundamental period.

6. Effect of material nonlinearities

In this section, period elongation due to yielding of infill plates is investigated. A similar technique explained in the previous section

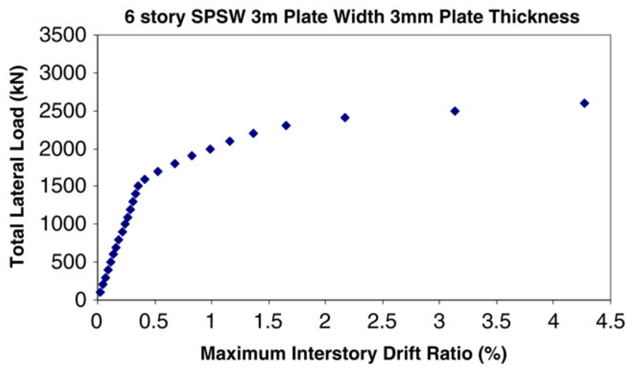

Fig. 9. A typical load versus maximum interstory drift ratio response for a SPSW.

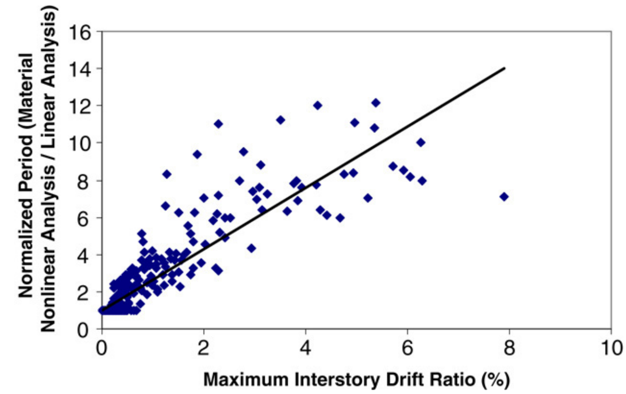

Fig. 10. Effects of material nonlinearities on fundamental period.

was used for this study. Twenty steel plate walls were considered and it was assumed that the infill plates are grade S235 [38] and boundary members are grade S355 [38] steel. As mentioned before capacity design principles were used in the design of these walls. AISC Seismic Provisions [22] mandate that the boundary elements remain elastic during seismic events. This recommendation was influential in selecting relatively stiff vertical boundary members. During a seismic event it is expected that the infill plates yield and behave as a ductile fuse while other elements display an elastic behavior. It was shown by Sabouri-Ghomi and others [3, 14] that when the infill plate yields, lateral forces are carried by the frame action of the boundary members. After plate yielding there is significant reduction in the lateral stiffness and this causes an elongation in the fundamental period. Period elongation is expected to be dependent on the level of inelasticity and on the stiffness of the boundary elements.

Usually natural periods of yielded systems are not of interest for structural designers. Designs are based on the original unyielded configuration. However, the amount of period elongation can be an indicator of the level of force reduction during seismic events. When a typical response spectrum is considered it is observed that the amount of base acceleration reduces as a function of the natural period in the constant velocity region.

Based on this discussion it is useful to quantify the amount of period elongation due to yielding of infill plates. In order to determine this relationship a series of prestressed buckling analysis was performed on steel plate walls. A particular wall was subjected to lateral loads in accordance with the first mode shape. The magnitude of these lateral forces was incremented. For a particular load level, the wall system was first analyzed by considering material nonlinearities. Lateral drifts at story levels were documented. Later, an eigenvalue analysis was performed to find out the natural period of the wall system. A typical plot of lateral load versus maximum interstory drift is given in Fig. 9. In this figure, each data point belongs to a separate analysis case.

All twenty walls were analyzed at various load levels by using the procedure explained above. Interstory drift was considered as an indicator of the level of inelasticity. For all analysis cases, the maximum interstory drift and the natural period were documented. Results are presented in Fig. 10 in normalized form. The final period values are normalized with respect to values from the analysis of the original unyielded configuration. It is obvious from this figure that there is significant amount of period elongation due to yielding of infill plates and this effect is much more pronounced for higher interstory drift levels. In order to quantify the amount of period elongation (T/T_w), a straight line is fitted to this data set and the following relationship is obtained.

$$\frac{T}{T_w} = 1.65ISD + 1 \qquad (19)$$

where, *ISD*: interstory drift ratio in percent.

This expression can be used to estimate the amount of period elongation as a function of the interstory drift. Eq. (19) was developed based on a limited amount of analysis on 20 SPSW details of which are given in Table 1. Design philosophies used other than the one adopted in this paper may result in the selection of different boundary members. The amount of period elongation is also expected to be influenced by the size of the boundary members. Similar expressions can be developed for other lateral load resisting systems and this can lead to comparisons among systems in terms of force reduction due to period elongation.

7. Conclusions

The fundamental natural period of steel plate shear wall systems is studied through numerical analysis. A class of structures which consist of walls and wall-frame systems was considered. This class of structures was analyzed by making use of the finite element method to obtain the fundamental natural period. Values obtained from numerical analysis are compared against the estimations provided in design specifications. A simple hand method is developed in this paper to estimate natural periods of steel walls and dual systems. Furthermore, the effects of geometrical and material nonlinearities on the fundamental natural period are investigated.

The following can be concluded from this study:

- Equations presented in design specifications for estimation of the fundamental period can lead to unsatisfactory results for some SPSW systems.
- The method developed in this paper is a simple and sufficiently accurate way of predicting the fundamental natural period of SPSW systems by hand calculation.
- Buckling of infill plates due to high slenderness results in an elongation of the period of the wall, but the extent of the elongation of the period is not significant. The effects of buckled infill plates can be neglected during the design of SPSW systems. An average elongation of 17% is observed for the wall systems investigated in this study.
- Yielding of infill plates due to lateral loads can significantly influence the amount of period elongation. A simple relationship was developed in this work to quantify the level of period elongation as a function of interstory drift for the wall systems investigated.
- The developed method is limited to structures that have uniform properties along the height. Further studies are required to extend this method to structures with variable stiffness properties.

Acknowledgements

This study was supported by a contract from The Scientific & Technological Research Council of Turkey (TÜBİTAK – 105M242).

Appendix

A.1. 4 Story SPSW Example (Case #9— Table 1)

$ptk = 3$ mm $\quad plw = 3000$ mm 150 tons/story

VBE(HD400 × 287) HBE(HEA300)

$I_{\mathrm{VBE}} = 99710 \times 10^4$ mm $^4 \quad A_{\mathrm{VBE}} = 366.3 \times 10^2$ mm^2

$d_{\mathrm{VBE}} = 393$ mm $\quad A_{fl} = 14600$ mm $^2 \quad A_{\mathrm{web}} = 8880$ mm ^{2}

$t_w = 22.6$ mm

$$H = 4 \times 3290 = 13160 \text{ mm} \qquad m = \frac{150000}{3290} = 45.6 \text{ kg/mm}$$

$$r_f = 0.812 \qquad E = 2 \times 10^8 \text{ kg}\frac{\text{mm}}{\text{s}^2}\frac{1}{\text{mm}^2}$$

$$Q_1 = 14600\,(0.5 \times 3000 + 393) = 27.64 \times 10^6 \text{ mm}^3$$

$$Q_2 = 27.64 \times 10^6 + 8880 \times 0.5\,(3000 + 393) = 42.70 \times 10^6 \text{ mm}^3$$

$$Q_3 = 366.3 \times 10^2 \times 0.5(3000 + 393) = 62.14 \times 10^6 \text{ mm}^3$$

$$Q_4 = 62.14 \times 10^6 + \frac{(3000)^2}{8}3 = 65.52 \times 10^6 \text{ mm}^3$$

$$\beta_1 = \frac{\left(27.64 \times 10^6\right)^2 + \left(42.7 \times 10^6\right)^2}{22.6}393 = 4.5 \times 10^{16} \text{ mm}^6$$

$$\beta_2 = \frac{\left(62.14 \times 10^6\right)^2 + \left(65.52 \times 10^6\right)^2}{2 \times 3}3000 = 4.08 \times 10^{18} \text{ mm}^6$$

$$\beta = 4.13 \times 10^{18} \text{ mm}^6$$

$$\begin{aligned} I_w &= \frac{3}{12}(3000)^3 + 2 \times 366.3 \times 10^2 \times (1697)^2 + 2 \times 99710 \times 10^4 \\ &= 2.2 \times 10^{11} \text{ mm}^4 \end{aligned}$$

$$KA_w = \frac{\left(2.2 \times 10^{11}\right)^2}{4.13 \times 10^{18}} = 11719 \text{ mm}^2$$

$$f_b = 0.812\frac{0.5595}{(13160)^2}\sqrt{\frac{2 \times 10^8 \times 2.2 \times 10^{11}}{4.56}} = 2.57 \text{ Hz}$$

$$f_s = 0.812\frac{1}{4 \times 13160}\sqrt{\frac{77 \times 10^6 \times 11719}{45.6}} = 2.17 \text{ Hz}$$

$$T_w = \sqrt{\frac{1}{(2.57)^2} + \frac{1}{(2.17)^2}} = 0.603 \text{ s}$$

$T_{FEM} = 0.563$ s (7% error).

A.2. 40 Story SPSW-Frame Example (Case #88— Table 2)

$ptk = 6$ mm $\quad plw = 6000$ mm 250 tons/story

HBE(HEA300)

Beams (HEA400) $\quad I_b = 45070 \times 10^4$ mm^4

VBE& Columns (HD400 × 347) $\quad L_b = 7000$ mm

$I_{\mathrm{VBE}} = 124900 \times 10^4$ mm$^4 \quad A_{\mathrm{VBE}} = 442 \times 10^2$ mm^2

$d_{\mathrm{VBE}} = 407$ mm $\quad A_{fl} = 17655$ mm$^2 \quad A_{\mathrm{web}} = 11150$ mm^2

$t_w = 27.2$ mm

$$H = 40 \times 3290 = 131600 \text{ mm} \qquad m = \frac{250000}{3290} = 76 \text{ kg/ mm}$$

$$r_f = 0.97 \qquad E = 2 \times 10^8 \text{ kg}\frac{\text{mm}}{\text{s}^2}\frac{1}{\text{mm}^2}.$$

Using a similar calculation procedure as in the previous example the following are found for the SPSW:

$$I_w = 1.02 \times 10^{12} \text{ mm}^4 \qquad KA_w = 41880 \text{ mm}^2 \qquad f_b = 0.051 \text{ Hz}$$

$$f_s = 0.38 \text{ Hz} \qquad T_w = 19.78 \text{ s}$$

$$I_{mw} = \frac{76 \times (131600)^4}{0.313 \times 0.97^2 \times 19.78^2 \times 2 \times 10^8} = 9.89 \times 10^{11} \text{ mm}^4$$

$$\begin{aligned} EI &= \left(9.89 \times 10^{11} + 4 \times 124900 \times 10^4\right) \times 2 \times 10^8 \\ &= 1.98 \times 10^{20} \text{ kg}\frac{\text{mm}}{\text{s}^2} \text{ mm}^2 \end{aligned}$$

$$K_{s1} = \frac{12 \times 2 \times 10^8}{3290\left[\frac{1}{\frac{4 \times 124900 \times 10^4}{3290}} + \frac{1}{\frac{2 \times 45070 \times 10^4}{7000}}\right]} = 8.66 \times 10^{10} \text{ kg}\frac{\text{mm}}{\text{s}^2}$$

$$r = \frac{6000}{2 \times 7000} = 0.428 \qquad \eta = \frac{6 \times 124900 \times 10^4 \times 7000}{45070 \times 10^4 \times 3290} = 35.38$$

$$s = \frac{35.38 - 3 \times 0.428 - 1}{35.38 + 2} = 0.89$$

$$\begin{aligned} K_{s2} &= 2\frac{6 \times 2 \times 10^8 \times 45070 \times 10^4}{7000 \times 3290} \\ &\quad \times [(1 + 0.428)\,(1 + 2 \times 0.428 + 0.89)] \\ &= 1.84 \times 10^{11} \text{ kg}\frac{\text{mm}}{\text{s}^2} \end{aligned}$$

$$K_{s1} + K_{s2} = 2.71 \times 10^{11}$$

$$\begin{aligned} I_g &= 442 \times 10^2\left[2 \times 3000^2 + 2 \times 10000^2 + 2 \times 17000^2\right] \\ &= 3.51 \times 10^{13} \text{ mm}^4 \end{aligned}$$

$$f_{fs}^2 = \frac{1}{(4 \times 131600)^2}\frac{0.97^2 \times 2.71 \times 10^{11}}{76} = 0.0121 \text{ Hz}^2$$

$$f_{fb}^2 = \frac{0.313 \times 0.97^2 \times 2 \times 10^8 \times 3.51 \times 10^{13}}{(131600)^4 \times 76} = 0.091 \text{ Hz}^2$$

$$\xi = \frac{0.091}{0.091 + 0.0121} = 0.88$$

$$K_s = 0.88 \times 2.71 \times 10^{11} = 2.38 \times 10^{11} \text{ kg}\frac{\text{mm}}{\text{s}^2}$$

$$\alpha = \sqrt{\frac{2.38 \times 10^{11}}{1.98 \times 10^{20}}} = 3.467 \times 10^{-5}\frac{1}{\text{mm}}\alpha H = 4.562$$

Exact $(\lambda_{sf}H)^2 = 9.3$ $\quad$ Approx. $(\lambda_{sf}H)^2 = 6.56$

$$T_{\mathrm{sys}} = \frac{2\pi\,(131600)^2}{9.3 \times 0.97}\sqrt{\frac{76}{1.98 \times 10^{20}}} = 7.47 \text{ s}$$

$T_{FEM} = 7.26$ s (2.8% error).

References

[1] Sabouri-Ghomi S, Roberts TM. Nonlinear dynamic analysis of thin steel plate shear walls. Computers and Structures 1991;39(1/2):121–7.
[2] Roberts TM, Sabouri-Ghomi S. Hysteretic characteristics of unstiffened perforated steel plate shear panels. Thin-Walled Structures 1992;14(2):139–51.
[3] Sabouri-Ghomi S, Roberts TM. Nonlinear dynamic analysis of steel plate shear walls including shear and bending deformations. Engineering Structures 1992;14(5):309–17.
[4] Roberts TM. Seismic resistance of steel plate shear walls. Engineering Structures 1995;17(5):344–51.
[5] Timler PA, Kulak GL. Experimental study of steel plate shear walls. Structural engineering report no. 114, Edmonton (Canada): Department of civil engineering, University of Alberta; 1983.
[6] Thorburn LJ, Kulak GL, Montgomery CJ. Analysis of steel plate walls. Structural engineering report no. 107, Edmonton (Canada): Department of civil engineering, University of Alberta; 1983.
[7] Tromposch EW, Kulak GL. Cyclic and static behavior of thin steel plate shear walls. Structural engineering report no. 145, Edmonton (Canada): Department of civil engineering, University of Alberta; 1987.
[8] Caccese V, Elgaaly M, Chen R. Experimental study of thin steel-plate shear walls under cyclic load. ASCE Journal of Structural Engineering 1993;119(2):573–87.
[9] Elgaaly M, Caccese V, Du C. Postbuckling behavior of steel-plate shear walls under cyclic loads. ASCE Journal of Structural Engineering 1993;119(2):588–605.
[10] Driver RG, Kulak GL, Kennedy DJL, Elwi AE. Cyclic test of four-story steel plate shear wall. ASCE Journal of Structural Engineering 1998;124(2):112–20.

[11] Driver RG, Kulak GL, Elwi AE, Kennedy DJL. FE and simplified models of steel plate shear wall. ASCE Journal of Structural Engineering 1998;124(2):121–30.
[12] Elgaaly M. Thin steel plate shear walls behavior and analysis. Thin Walled Structures 1998;32:151–80.
[13] Lubell AS, Prion HGL, Ventura CE, Rezai M. Unstiffened steel plate shear wall performance under cyclic loading. ASCE Journal of Structural Engineering 2000;126(4):453–60.
[14] Sabouri-Ghomi S, Ventura CE, Kharrazi MHK. Shear analysis and design of ductile steel plate walls. ASCE Journal of Structural Engineering 2005;131(6): 878–89.
[15] Park HG, Kwack JH, Jeon SW, Kim WK, Choi IR. Framed steel plate wall behavior under cyclic lateral loading. ASCE Journal of Structural Engineering 2007; 133(3):378–88.
[16] Berman J, Bruneau M. Plastic analysis and design of steel plate shear walls. ASCE Journal of Structural Engineering 2003;129(11):1448–56.
[17] ASCE 7. Minimum design loads for buildings and other structures. American Society of Civil Engineers, Structural Engineering Institute, USA; 2005.
[18] Eurocode 8. Design of structures for earthquake resistance. Part 1. Brussels: CEN (European Committee for Standardization); 2003.
[19] National Building Code of Canada, Canadian Commission on Building and Fire Codes, National Research Council of Canada, Ottawa, Ontario; 2005.
[20] Goel RK, Chopra AK. Period formulas for concrete shear wall buildings. ASCE Journal of Structural Engineering 1998;124(4):426–33.
[21] Tremblay R. Fundamental periods of vibration of braced steel frames for seismic design. Earthquake Spectra 2005;21(3):833–60.
[22] AISC. Seismic Provisions for Structural Steel Buildings, Chicago, Illinois; 2005.
[23] AISC. Specification for Structural Steel Buildings, Chicago, Illinois; 2005.
[24] ANSYS. Version 8.1 On-line User's Manual; 2006.
[25] Chopra AK. Dynamics of structures — Theory and applications to earthquake engineering. New Jersey: Prentice Hall; 1995.
[26] Timoshenko S, Young DH. Vibration problems in engineering. third ed. New Jersey: D. Van Nostrand Company Inc.; 1955.
[27] Karnovsky IA, Lebed OI. Formulas for structural dynamics. McGraw Hill; 2001.
[28] Blevins RD. Formulas for natural frequency and mode shape. Florida: Krieger Publishing Co; 1979.
[29] Zalka KA. A simplified method for calculation of the natural frequencies of wall-frame buildings. Engineering Structures 2001;(23):1544–55.
[30] Ugural AC, Fenster SK. Advanced strength and applied elasticity. 4th ed. New Jersey: Prentice Hall; 2003.
[31] Atasoy M. Lateral stiffness of unstiffened steel plate shear walls. MS thesis. Ankara, Turkey: Middle East Technical University; 2008.
[32] Heidebrecht AC, Smith BS. Approximate analysis of tall wall-frame structures. Journal of the Structural Division, Proceedings of the American Society of Civil Engineers 1973;99(2):199–221.
[33] Smith BS, Crowe E. Estimating periods of vibration of tall buildings. ASCE Journal of Structural Engineering 1986;112(5):1005–19.
[34] Rutenberg A. Approximate natural frequencies for coupled shear walls. Earthquake Engineering and Structural Dynamics 1975;4:95–100.
[35] Chrysanthakopoulos C, Bazeos N, Beskos DE. Approximate formulae for natural periods of plane steel frames. Journal of Constructional Steel Research 2006; 62:592–604.
[36] Wagner H. Flat sheet metal girders with very thin webs, Part I- General theories and assumptions. Tech. Memo. No. 604, National Advisory Committee for Aeronautics, Washington DC; 1931.
[37] Behbahanifard MR, Grondin GY, Elwi AE. Experimental and numerical investigation of steel plate shear wall. Structural Engineering Report 254, Department of Civil and Environmental Engineering, University of Alberta; 2003.
[38] EN 10025. Hot rolled products of non-alloy structural steel. CEN, European Committee for Standardization, Brussels; 1994.